

Laser Flash Photolysis of Arylsulfonium Salts: Studies of Photoproduced Proton Kinetics and Mechanism in Polar Solvents by a pH-Jump Method

Kai-Kong Iu, Joe Kuczynski,[†] S. J. Fuerniss,[‡] and J. Kerry Thomas*

Contribution from the Department of Chemistry and Biochemistry, University of Notre Dame, Notre Dame, Indiana 46556. Received December 16, 1991.

Revised Manuscript Received February 28, 1992

Abstract: Nanosecond time-resolved laser spectroscopy was employed as a tool to study the kinetics and mechanism of photoproduced protons on the quenching of excited arenes with triphenylsulfonium and (3-(9-anthracenyl)propyl)diphenylsulfonium hexafluoroantimonate in acetonitrile and methanol. Triphenylsulfonium hexafluoroantimonate quenches singlet excited pyrene and anthracene via an electron-transfer mechanism, with a quenching rate constant of the order of $10^{10} \text{ M}^{-1} \text{ s}^{-1}$. Electron transfer from singlet excited anthracene to triphenylsulfonium hexafluoroantimonate and direct excitation of (3-(9-anthracenyl)propyl)diphenylsulfonium hexafluoroantimonate in acetonitrile both create an in-cage phenyl rearranged cationic transitory species with an excess proton ($\text{Ph-An}(\text{H}^+)$), which absorbs at around 490 nm and has a half-life of microseconds under anhydrous condition. In the case of direct excitation of (3-(9-anthracenyl)propyl)diphenylsulfonium hexafluoroantimonate in acetonitrile, the in-cage rearranged cationic transient can be quenched by I^- ion and water with a quenching rate of $(2.53 \pm 0.45) \times 10^{10}$ and $(3.95 \pm 0.70) \times 10^6 \text{ M}^{-1} \text{ s}^{-1}$, respectively. The homolytic cleavage product such as Ph_2S^{++} is observed neither on electron transfer from singlet excited arene (i.e., $^1\text{An}^*$ or $^1\text{Py}^*$) nor on direct excitation. The quantum yields of photoproduced protons with (3-(9-anthracenyl)propyl)diphenylsulfonium hexafluoroantimonate are 0.9 ± 0.1 in methanol and 0.4 ± 0.05 in acetonitrile. The dye sodium bromocresol green was used as a proton acceptor in pH-jump experiments, where the rate of photoproduced protons was measured by photobleaching of the dye at 620 nm. The results reveal that the photoproduced proton rate is about $10 \mu\text{s}$ (half-life) in acetonitrile under anhydrous conditions and matches the decay of the transitory species, which exhibits a λ_{max} at 490 nm. However, the rate of proton formation is increased in the presence of water. The photoproduced proton rate is very fast in methanol (e.g., $<200 \text{ ns}$).

Introduction

In industry, triarylsulfonium salts are employed extensively in photoinduced polymerization processes.¹ The salts exhibit the unique character of generating protons on exposure to UV radiation. Several studies of triarylsulfonium salt photochemistry have been compiled² over the last decade. Basically, the singlet excited state of triphenylsulfonium cation decomposes either homolytically or heterolytically to yield products of homolytic cleavage, which are Ph_2S^{++} and Ph^+ , and products of heterolytic cleavage, which are Ph_2S and Ph^+ . Further reactions of these species with the solvent produce protons. For the aryl-substituted sulfonium cation, in-cage singlet rearrangement often occurs and generates a variety of derivatives of diaryl sulfide.³ However, in-cage rearrangement products such as phenylthiobiphenyl isomers can be eliminated by triplet sensitization ($k_T > 75 \text{ kcal/mol}$), which produces triplet dissociation products such as Ph_2S^{++} and Ph^+ .⁴

Unfortunately, most of the photochemical studies of triarylsulfonium salts have relied on product analysis. Kinetic information, such as the photoproduced protons rate, or direct detection of short-lived intermediates is often lacking. Here, we employ nanosecond time-resolved laser spectroscopy and a pH-jump method⁵ to investigate short-lived transitory species on photolysis of triarylsulfonium salts.

Experimental Section

Chemicals. All solvents (spectral or anhydrous, 99+%) were purchased from Aldrich; anthracene (gold label) and pyrene (99%) were also obtained from Aldrich. The purification of pyrene had been described elsewhere.⁶ High-purity grade triphenylsulfonium hexafluoroantimonate and (3-(9-anthracenyl)propyl)diphenylsulfonium hexafluoroantimonate⁷ were supplied by IBM Corp. and were used as received. Bromocresol green was purchased from Aldrich and recrystallized twice from methanol, the sodium salt of bromocresol green was prepared by neutralization with NaOH_{aq} , and the water was then removed by evacuation to obtain the dry sodium salt.

Time-Resolved Laser Flash Spectrometry. Either a PRA LN100 nitrogen laser (1 ns, 337 nm, 60 μJ) or a Continuum PY-61 YAG laser (3rd harmonics, 355 nm, 20 ps, 6 mJ) was used as the excitation source for the time-resolved fluorescence studies (i.e., 337 nm for pyrene; 355 nm for anthracene). The absorbance of the arene sample at the excitation wavelength was 0.8 ± 0.05 . The fluorescence of the arene (i.e., 400 nm for pyrene; 410 nm for anthracene) was collected through a lens system and passed through a Bausch & Lomb monochromator equipped with a UV grating (1350 lines/mm, blazed at 400 nm). The monochromator slit width was set to a 2-nm band pass for all the experiments. The fluorescence light was detected by a multichannel plate photomultiplier (Hamamatsu R1664U). The analog signal from the PMT was subsequently transferred to an IBM PC-AT compatible computer (Zenith Z-386) through a 750-MHz wave-form digitizer (Tektronix 7912HB) for further data processing. The response of the whole detection system was $\sim 500 \text{ ps}$.

A Lambda Physik Model EMG100 nitrogen (6 ns, 337 nm, 5 mJ) laser was used as the excitation source for transient absorption experiments. A pulsed 450-W Xe lamp with a (PRA Model 301/302) power supply and a pulsing unit (PRA Model M-305) was employed as the analyzing light source. The Xe light pulse from this pulsing unit provides a flat baseline pulse up to 150 μs . The white light from the Xe lamp was passed through a UV cutoff filter (KOPP glass Inc., Model 3-75) to avoid bleaching of the ground state of the arene. The analyzing probe light from the sample was collected by a lens system and guided to the entrance slit of a Bausch & Lomb monochromator with a visible grating

(1) (a) Crivello, J. V.; Conlon, D. A. *Makromol. Chem. Macromol. Symp.* **1988**, 13-14, 145-160. (b) Crivello, J. V. *Adv. Polym. Sci.* **1984**, 62, 1-48. (c) Crivello, J. V. *Dev. Polym. Photochem.* **1981**, 2, 1-38. (d) Roffery, C. G. *Photopolymerization of Surface Coatings*; Wiley: New York, 1982.

(2) Dektar, J. L.; Hacker, N. P. *J. Am. Chem. Soc.* **1990**, 112, 6004-6015 and references cited therein.

(3) (a) Saeva, F. D.; Morgan, B. P.; Luss, H. R. *J. Org. Chem.* **1985**, 50, 4360-4362. (b) Dektar, J. L.; Hacker, N. P. *J. Chem. Soc., Chem. Commun.* **1987**, 1591-1592. (c) Saeva, F. D.; Breslin, D. T. *J. Org. Chem.* **1989**, 54, 712-714.

(4) Dektar, J. L.; Hacker, N. P. *J. Org. Chem.* **1988**, 53, 1833-1835.

(5) (a) Gutman, M.; Huppert, D.; Pines, E. *J. Am. Chem. Soc.* **1981**, 103, 3709-3713. (b) Clark, J. H.; Shapiro, S. L.; Campillo, A. J.; Winn, K. R. *J. Am. Chem. Soc.* **1979**, 101, 746-748.

(6) Iu, K.-K.; Thomas, J. K. *Langmuir* **1990**, 6, 471-478.

(7) Angelo, R. W.; et al. U.S. Patent 5,047,568, 1991.

* Author to whom correspondence should be addressed.

[†] IBM Corp., Entry Systems Technology Division, Boca Raton, FL 33432.

[‡] IBM Corp., Systems Technology Division, Endicott, NY 13760.

Table I. Photoproduced Proton Quantum Yield of (3-(9-Anthracenyl)propyl)diphenylsulfonium Hexafluoroantimonate in Polar Solvent

solvent	quantum yield
methanol	0.90 ± 0.10
CH ₃ CN	0.40 ± 0.05

Table II. Ph₃SSbF₆ Quenching Rate Constants of Arene^a Fluorescence in Acetonitrile Solution

arene	time-resolved, × 10 ⁻¹⁰ M ⁻¹ s ⁻¹	Stern-Volmer, × 10 ⁻¹⁰ M ⁻¹ s ⁻¹
pyrene	1.02 ± 0.04	1.30 ± 0.04
anthracene	1.16 ± 0.06	1.25 ± 0.09

^aSee Experimental Section.

(1350 lines/mm, blazed at 500 nm). The monochromator slit width was set to a 2-nm band pass for all the experiments. A master triggering unit was used to control triggering of the digitizer and the pulsing unit of the Xe lamp. A Hamamatsu R-928 red-sensitive PMT with a variable load resistor was used to detect the optical signal. A Tektronix 7A13 differential amplifier was used to offset the background voltage. The fastest RC response of this system is about 5 ns.

Steady-State Measurements and Photoproduct Isolation. An SLM Instruments Inc. spectrofluorometer, Model SPF500C, equipped with a 250-W Xe lamp and a Hamamatsu R-928 red-sensitive PMT used as photodetector, was used for steady-state fluorescence studies. The spectrofluorometer was interfaced to a Zenith Z-386 IBM PC-AT compatible computer. The excitation and emission band pass for all fluorescence spectra and Stern-Volmer studies were 2 and 1 nm, respectively. A Beckman Cary-3 UV-vis spectrometer interfaced to a Zenith Z-386 IBM PC-AT compatible computer was used for collecting steady-state UV-vis spectra. A Waters Model 501 HPLC equipped with a C₁₈ column and a spectrophotometer (Waters Model 481) was used to isolate the photoproducts.

The quantum yield of photoproduced proton production was measured by photolyzing a 3 mM solution of (3-(9-anthracenyl)propyl)diphenylsulfonium hexafluoroantimonate solution with selected light in a SLM fluorometer for 10 min at 375 nm (band pass = 10 nm). The percentage of photodecomposition was less than 5% of the sulfonium salt. The power of the photolyzing light source was measured by a power meter (Science Tech Inc. Model 380101). The photolyzed solution, 0.5 mL, was then mixed with 10 mL of a 2.5 × 10⁻⁵ M sodium bromocresol green aqueous solution. The mixture comes to equilibrium as follows: $\text{HIn} \rightleftharpoons \text{H}^+ + \text{In}^-$.

The concentration of In⁻ was determined by its spectral absorption at 620 nm ($A_{620\text{nm}}, \epsilon_{620} = 3.38 \times 10^4 \text{ cm}^{-1} \text{ M}^{-1}$) and the equilibrated [HIn] was calculated by subtracting the [In⁻] from the initial concentration of sodium bromocresol green used. The equilibrium [H⁺] was calculated by using $\text{p}K_a = 4.78$ for bromocresol green in water. The results are listed in Table I.

Results and Discussions

Transitory Species and Rate Data. Figure 1 shows the quenching of pyrene fluorescence by Ph₃SSbF₆ in acetonitrile solution. Figure 1A is the time-resolved pyrene fluorescence signal at 400 nm with different [Ph₃SSbF₆] and the smooth curve on the data is a single-exponential decay fitting function expressed as

$$I = I_0 \exp(-k_{\text{obs}}t) \quad (1)$$

where I is the fluorescence intensity at any time (t), I_0 is the fluorescence intensity right after the laser flash, and k_{obs} is the decay rate constant of the signal. This observed decay rate constant is a pseudo-first-order rate constant and can be rewritten as eq 2, where k_0 is the fluorescence decay rate constant at zero

$$k_{\text{obs}} = k_0 + k_q[\text{Ph}_3\text{SSbF}_6] \quad (2)$$

quencher concentration and k_q is the quenching rate constant for the various [Ph₃SSbF₆] in our studies. The decay rate constants (k_{obs}) from the fits are plotted as a function of [Ph₃SSbF₆] as shown in Figure 1B. The slope of the linear least-square fit line in Figure 1B is equal to k_q . Figure 1C is the standard steady-state

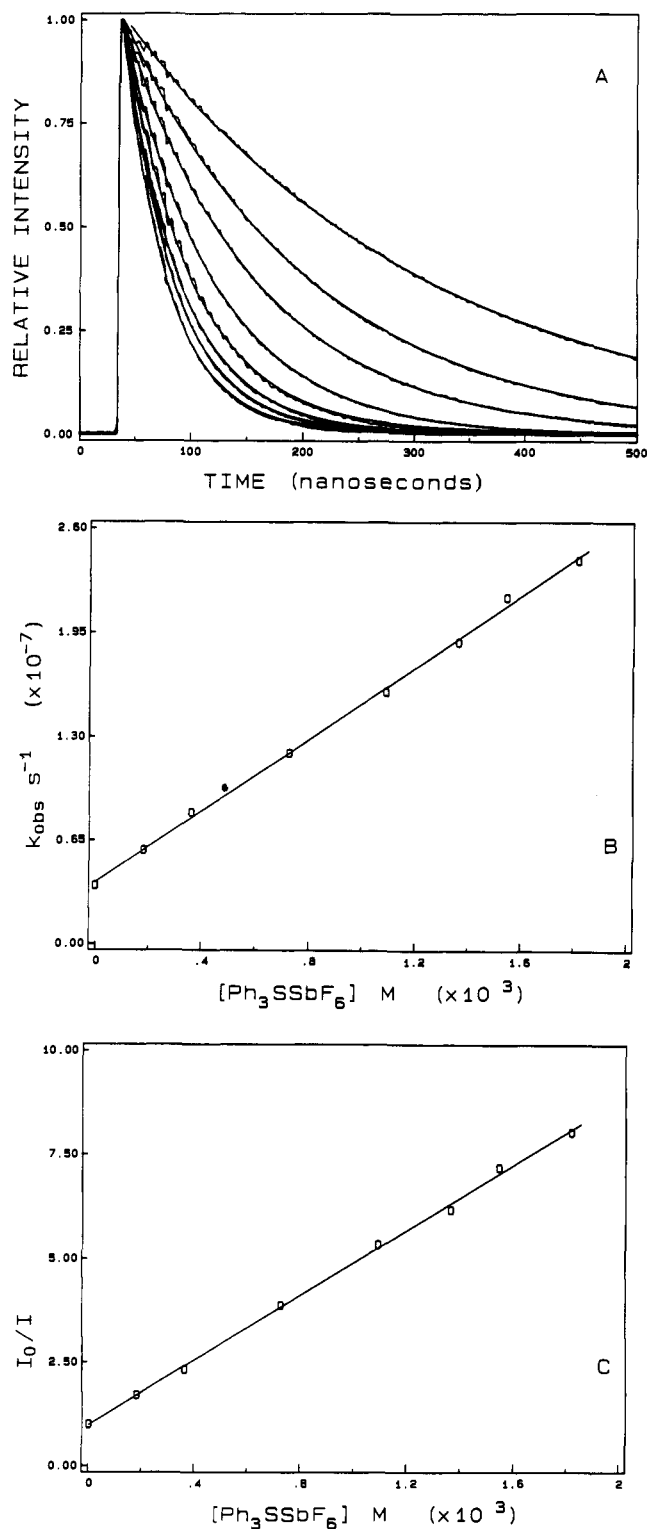


Figure 1. Quenching of pyrene fluorescence by Ph₃SSbF₆ in CH₃CN solution. (A) Time-resolved pyrene fluorescence decay at different [Ph₃SSbF₆], smooth curve through the data is a single-exponential function fit. Starting from slowest decay, the [Ph₃SSbF₆] were 0, 2.0 × 10⁻⁴, 4.0 × 10⁻⁴, 8.0 × 10⁻⁴, 1.2 × 10⁻³, 1.5 × 10⁻³, 1.7 × 10⁻³, and 2.0 × 10⁻² M. (B) Least-square linear fit of the observed decay rate in (A) as a function of [Ph₃SSbF₆]. (C) Least-square linear fit of the steady-state pyrene fluorescence intensity as a function of [Ph₃SSbF₆], a Stern-Volmer plot.

Stern-Volmer plot, where I and I_0 are the fluorescence intensities with and without Ph₃SSbF₆, respectively. The relationship between I_0/I and [Ph₃SSbF₆] is described by the Stern-Volmer equation⁹

$$I_0/I = 1 + k_q\tau_0[\text{Ph}_3\text{SSbF}_6] \quad (3)$$

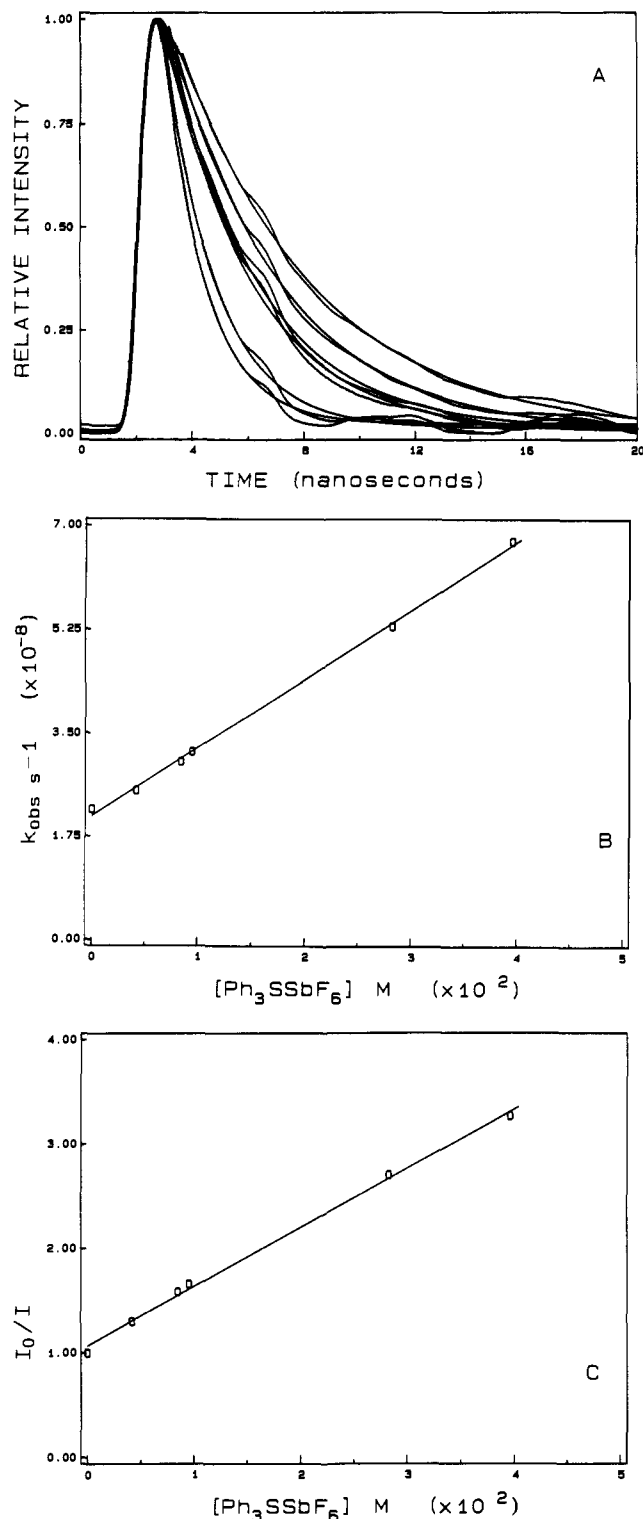


Figure 2. Quenching of anthracene fluorescence by Ph_3SSbF_6 in CH_3CN solution. (A) Time-resolved anthracene fluorescence decay at different $[Ph_3SSbF_6]$, smooth curve through the data is a single-exponential function fit. Starting from slowest decay, the $[Ph_3SSbF_6]$ were 0 , 4.2×10^{-3} , 8.5×10^{-3} , 9.5×10^{-3} , 2.8×10^{-2} , and 4.0×10^{-2} M. (B) Least-square linear fit of the observed decay rate in (A) as a function of $[Ph_3SSbF_6]$. (C) Least-square linear fit of the steady-state anthracene fluorescence intensity as a function of $[Ph_3SSbF_6]$, a Stern-Volmer plot.

where τ_0 is the reciprocal of k_0 .

Figure 2 shows the same kind of plot as in Figure 1, but the

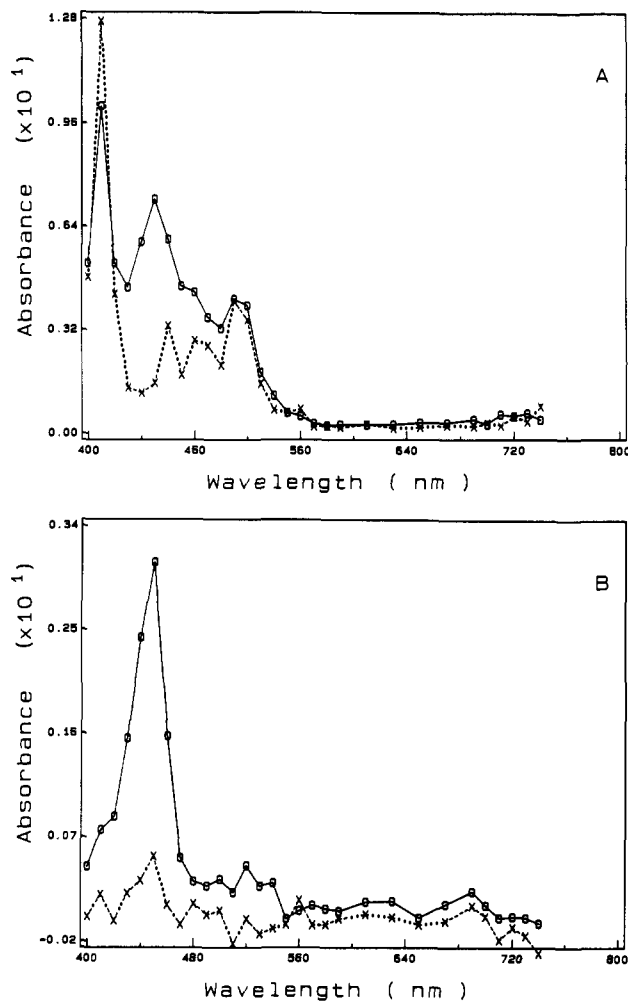


Figure 3. Transient absorption spectrum of pyrene and Ph_3SSbF_6 in CH_3CN solution. (O, solid line) 5×10^{-5} M pyrene and 3×10^{-3} M Ph_3SSbF_6 ; (X, dashed line) 5×10^{-5} M pyrene only. (A) Spectra taken 200 ns after the laser flash. (B) Spectra taken $3 \mu s$ after the laser flash.

arene is anthracene instead of pyrene. The results of the k_q obtained from both experiments for anthracene and pyrene are listed in Table II. Our results of the quenching rate k_q agree with the data of DeVoe et al.^{18a} (i.e., $k_q = 1.4 \times 10^{10} M^{-1} s^{-1}$ for Ph_3SPF_6).

Figure 3A shows a comparison of the transient absorption spectrum of air-saturated pyrene/ CH_3CN with and without Ph_3SSbF_6 taken 200 ns after the laser flash. For the system pyrene/ CH_3CN itself, the spectrum shows only $^3Py^*$ (410 and

(10) We would like to thank one of the reviewers comments on our earlier assignment of the ground-state CT complex that might cause a nonlinear plot on Stern-Volmer measurement. (a) Keizer, J. *J. Am. Chem. Soc.* **1983**, *105*, 1494-1498. (b) Kusumoto, Y.; Ihara, S.; Kurawaki, J.; Satake, I. *Chem. Lett.* **1986**, *10*, 1647-1650.

(11) Kikuchi, K. *JOEM Handbook 1, Triplet-triplet Absorption Spectra*; Bunshin: Tokyo, 1989; p 155.

(12) Shida, T. *Physical Sciences Data 34, Electronic Absorption Spectra of Radical Ions*; Elsevier: New York, 1988; p 86.

(13) Reference 11, p 51.

(14) Reference 12, p 69.

(15) Kazuuda, K.; Thomas, J. K. *J. Chem. Soc., Faraday Trans.* **1992**, *88*, 195-200.

(16) Reference 12, p 386.

(17) Pappas, S. P.; Pappas, B. C.; Gatechair, L. R.; Jilek, J. H.; Schnabel, W. *Polym. Photochem.* **1984**, *5*, 1.

(18) (a) DeVoe, R. J.; Sahyun, M. R. V.; Schmidt, E.; Serpone, N.; Sharma, D. K. *Can. J. Chem.* **1988**, *66*, 319-324. (b) Dektar, J. L.; Hacker, N. P. *Photochem. Photobiol. A* **1989**, *46*, 233-238.

(19) Wendt, H.; Hoffelner, H. *Electrochem. Acta* **1983**, *28*, 1453.

(20) Pysh, E. S.; Yang, N. C. *J. Am. Chem. Soc.* **1963**, *85*, 2124-2130.

(9) Stern, I.; Volmer, M. *Physik. Z.* **1919**, *20*, 183.

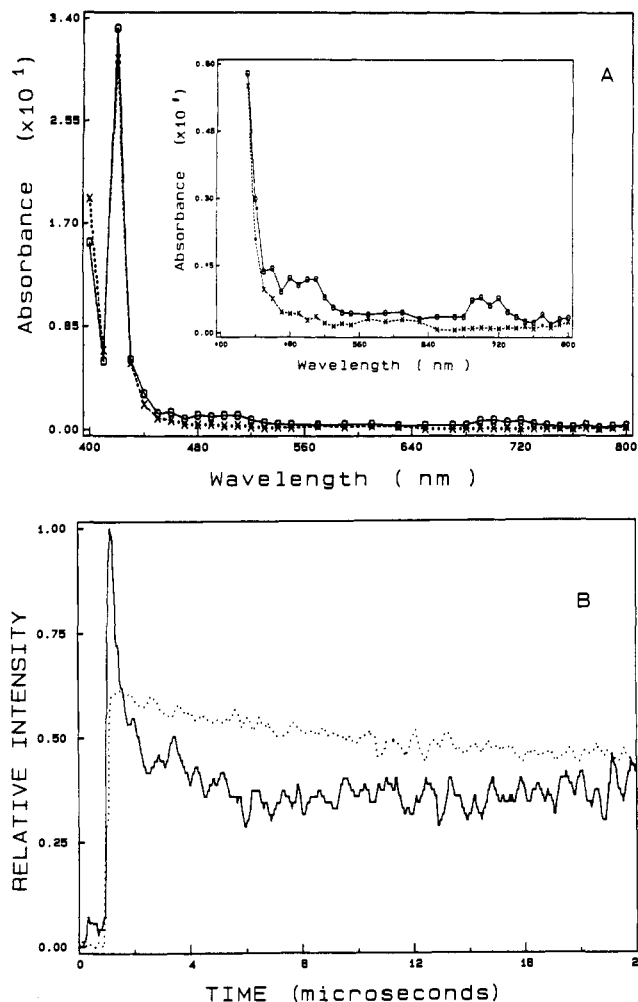


Figure 4. (A) Transient absorption spectra of anthracene and Ph_3SSbF_6 in CH_3CN solution. (O, solid line) 2.2×10^{-4} M anthracene and 8×10^{-3} M Ph_3SSbF_6 ; (X, dashed line) 2.2×10^{-4} M anthracene only. Spectra taken 200 ns after the laser flash. Insert shows expanded scale in the 440–800-nm regime. (B) Time-resolved signal of 2.2×10^{-4} M anthracene and 8×10^{-3} M Ph_3SSbF_6 : solid line, 490 nm; dotted line, 700 nm.

510 nm)¹¹ and a small yield of Py^{++} (450 nm);¹² however, the Py^{++} absorption at 450 nm markedly increases if 3 mM Ph_3SSbF_6 is added to the system. The formation of Py^{++} in the pyrene- Ph_3SSbF_6 sample is confirmed by retaking the transient absorption spectrum after a longer delay (3 μs); a distinct peak at 450 nm, which is due to the Py^{++} absorption, is observed for the pyrene- Ph_3SSbF_6 sample and it is shown in Figure 3B.

Because of the strong absorption of ${}^3\text{Py}^*$ and Py^{++} in the 450–550-nm spectral region, any weak absorption originating in other species is not easily detected in the 450–500-nm region. Hence, anthracene was used in place of pyrene, and the transient absorption studies are repeated to give the spectrum shown in Figure 4A taken 200 ns after the laser flash. The scale of the insert of Figure 4A has been expanded between 440 and 800 nm and reveals the presence of species other than ${}^3\text{An}^*$ (420 nm)¹³ and An^{++} (700 nm).¹⁴ Figure 4B shows the time-resolved signal at 490 and 700 nm. The initial falloff of the 490-nm (solid line) species is much faster than that of An^{++} at 700 nm (dotted line); this suggests that the species absorbing at 490 nm (a cationic transience, vide infra) is not An^{++} (also see Figure 5B).

Figure 5A shows the transient absorption spectrum of (3-(9-anthracenyl)propyl)diphenylsulfonium hexafluoroantimonate in CH_3CN with and without iodide ion—an efficient cation quencher. The spectrum with I^- (5.2×10^{-3} M) shows only the anthracene-derived triplet excited state at 420 nm; in contrast, the spectrum without I^- has an additional broad absorption band at 490 nm in addition to the triplet excited state at 420 nm and the

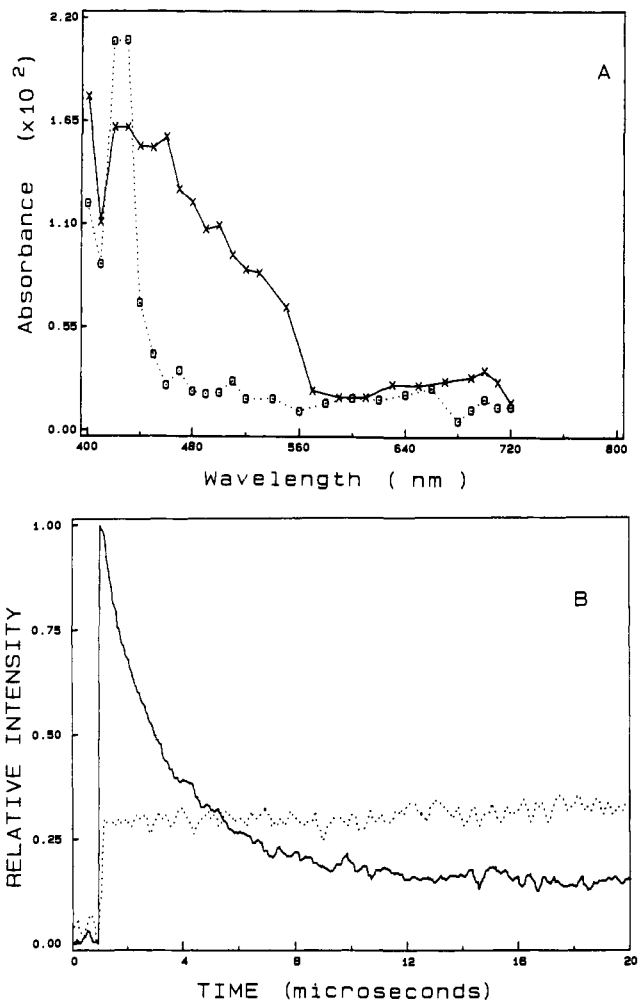


Figure 5. (A) Transient absorption spectrum of (3-(9-anthracenyl)propyl)diphenylsulfonium hexafluoroantimonate in CH_3CN (3.35×10^{-4} M) solution with (O, dotted line) and without (X, solid line) 5.2×10^{-3} M KI. Spectra taken 200 ns after the laser flash. (B) Time-resolved signal of (3-(9-anthracenyl)propyl)diphenylsulfonium hexafluoroantimonate in CH_3CN : solid line, 490 nm; dotted line, 700 nm.

Table III. Quenching Rate Constants of the 490-nm Transient Absorption Signal of (3-(9-Anthracenyl)propyl)diphenylsulfonium Hexafluoroantimonate in Acetonitrile Solution^a

quencher	$k_q, \text{M}^{-1} \text{s}^{-1}$
I^-	$(2.53 \pm 0.45) \times 10^{10}$
H_2O	$(3.95 \pm 0.70) \times 10^6$

^a The concentration of the sulfonium salt was 2×10^{-4} M.

radical cation at 700 nm. Because I^- is a very effective cation quencher (e.g., k_q for $\text{Py}^{++} = 3 \times 10^{10} \text{M}^{-1} \text{s}^{-1}$ in methanol¹⁵) and the fact that oxygen has no effect on this 490-nm absorption signal, it is suggested that this species is cationic. It is interesting to note that the triplet absorption peak increases in the sample with I^- and is probably due to the heavy-atom effect (enhanced intersystem crossing) caused by iodide. Figure 5B shows the time-resolved signal at 490 and 700 nm similar to that in Figure 4B. Again, data suggest that this species absorbed at around 490 nm is a cation quenched rapidly by I^- and is not An^{++} .

Figure 6 shows the pseudo-first-order quenching of the 490-nm species by H_2O and I^- , the treatment of the observed decay rate is the same as in eq 2. The quenching rate from the slope is listed in Table III. The quenching rate of iodide ion is $(2.53 \pm 0.45) \times 10^{10} \text{M}^{-1} \text{s}^{-1}$, which is similar to the quenching rate of radical cations by iodide ion.¹⁵

pH-Jump Measurements. Figure 7 shows the effect of water on the cationic absorption signal at 490 nm and on the photobleaching of sodium bromocresol green (pH indicator) at 620 nm.

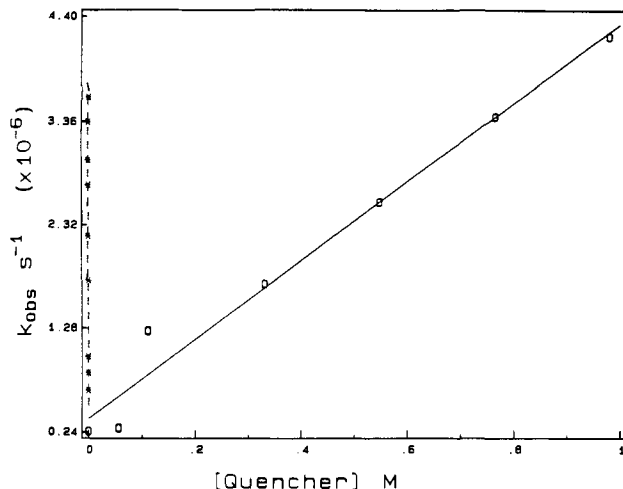


Figure 6. Least-square linear fit of the 490-nm transient absorption signal decay rate as a function of quencher: (O, solid line) H₂O; (*, dashed line) KI.

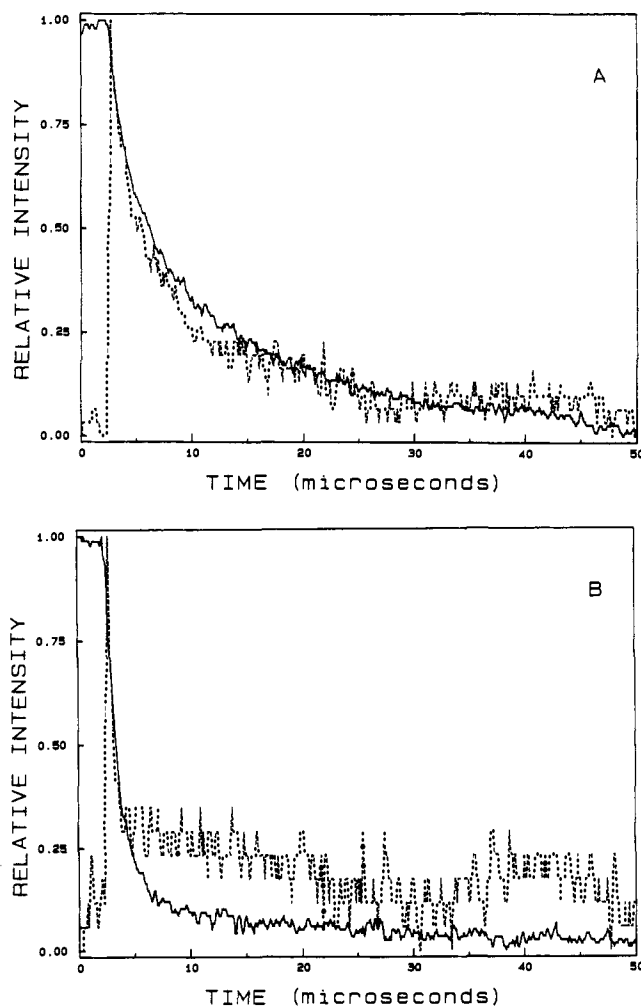


Figure 7. Time-resolved transient signal of 3.37×10^{-4} M (3-(9-anthracenyl)propyl)diphenylsulfonium hexafluoroantimonate in CH₃CN. (A) Anhydrous solution: (solid line) photobleaching at 620 nm, solution contained 5×10^{-5} M sodium bromocresol green; (dashed line) absorption signal at 490 nm. (B) Same description as (A) but 2% H₂O (1.1 M) was added to the sample solution.

The photobleaching at 620 nm of sodium bromocresol green is due to the bleaching of the [In⁻] by reaction with the photoproducted protons to form HIn. Figure 7A is (3-(9-anthracenyl)propyl)diphenylsulfonium hexafluoroantimonate in anhydrous (H₂O < 0.005%) CH₃CN. The solid line is the 620-nm time-

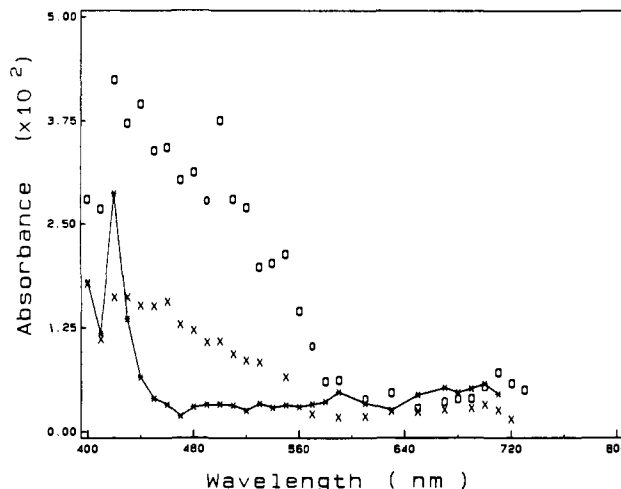


Figure 8. Transient absorption spectrum of (3-(9-anthracenyl)propyl)diphenylsulfonium hexafluoroantimonate in different solvents taken 200 ns after the laser flash: (O) in benzonitrile; (X) in acetonitrile (same as in Figure 5A); (*, line) in methanol.

resolved dye-photobleaching signal with 5×10^{-5} M dye; the dashed line is the 490-nm cationic absorption signal. Figure 7B shows data similar to those in Figure 7A, but with addition of 2% water ([H₂O] = 1.1 M) in the samples. The excellent matching of the decay of the 490-nm absorption signal with the bleaching rate of the 620-nm dye photobleaching signal indicates that the photoproducted proton is related to the decay of the cationic species, which absorbs at 490 nm.

Figure 8 shows the transient spectrum on excitation of (3-(9-anthracenyl)propyl)diphenylsulfonium hexafluoroantimonate in different solvents. Basically, the spectra in acetonitrile and benzonitrile are similar, and a distinct broad absorption band at 490 nm is observed in both solvents. The spectrum in methanol, however, is different from that in either acetonitrile or benzonitrile, and the broad band at 490 nm is absent. It is pertinent to note that electron transfer from ¹An* to Ph₃SSbF₆ in acetonitrile also shows a similar spectrum (Figure 4) to that in Figure 8. The 490-nm absorption species is assigned to a Ph-An(H⁺) cation (vide infra).

Product Analysis. Figure 9A shows the steady-state fluorescence spectra of the photolysis products of (3-(9-anthracenyl)propyl)diphenylsulfonium hexafluoroantimonate in acetonitrile. The first fraction of the HPLC separation (see Experimental Section) shows characteristics of 9-alkylated anthracene derivatives and the fourth fraction shows characteristics of 9-phenylated anthracene derivatives.²¹ These characteristics are that the relative fluorescence intensity at >420 nm is larger in 9-phenylated anthracene and the fluorescence lifetime is longer in 9-phenylated anthracene. Figure 9B shows the time-resolved fluorescence signal of these two fractions. The decay time of the first fraction is 3 ns and the decay time of the fourth fraction is 8 ns; these lifetimes are identical with those of 9-alkylated and 9-phenylated anthracene, respectively.²¹ In addition, the retention times of the two fraction are identical with those of the model compound (e.g., 9-methyl- and 9-phenylanthracene). Excitation of the An chromophore in (3-(9-anthracenyl)propyl)diphenylsulfonium hexafluoroantimonate salt gives an anthracene fluorescence that has a much shorter lifetime (<1 ns) than that of anthracene (3 ns). This is due to quenching of the excited An chromophore by the sulfonium group. The reaction is electron transfer to the cationic group.

Figure 10 shows a photobleaching signal at 620 nm of (3-(9-anthracenyl)propyl)diphenylsulfonium hexafluoroantimonate with sodium bromocresol green in methanol. Comparing these data to those in Figure 7 reveals that the rate of production of pho-

(21) Berlman, I. B. *Handbook of fluorescence spectra of aromatic molecule*, 2nd ed.; Academic: New York, 1971; pp 358, 363, and 364.

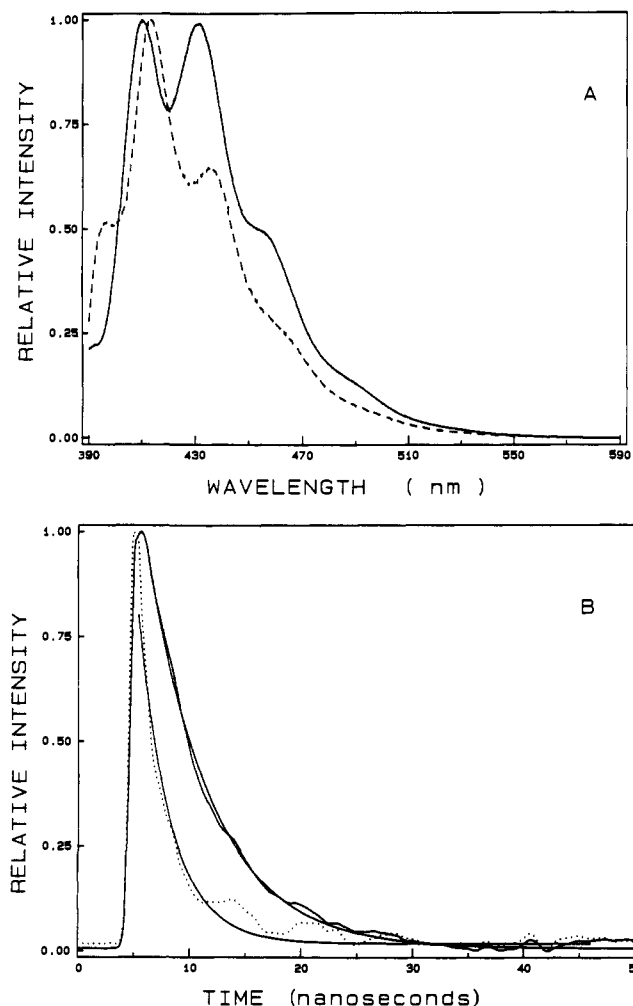


Figure 9. Fluorescence of fractions 1 and 4 after HPLC separation. (A) Steady-state spectrum excited at 380 nm: (dashed line) first fraction; (solid line) fourth fraction. (B) Time-resolved fluorescence: (solid line with long decay) fourth fraction; (dotted line with short decay) first fraction. The smooth curve on the signal is a calculated single-exponential decay function.

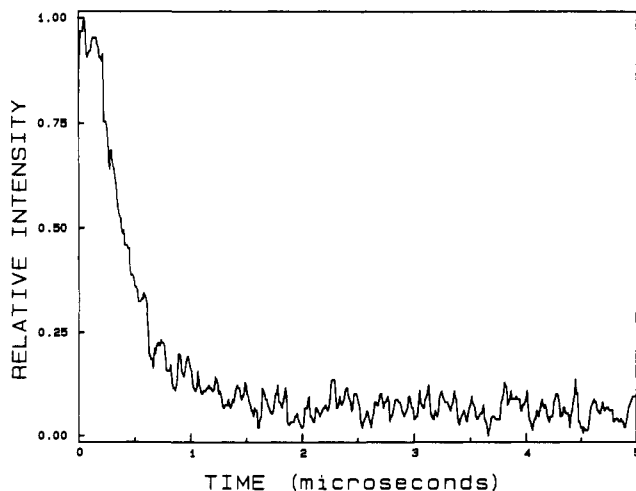
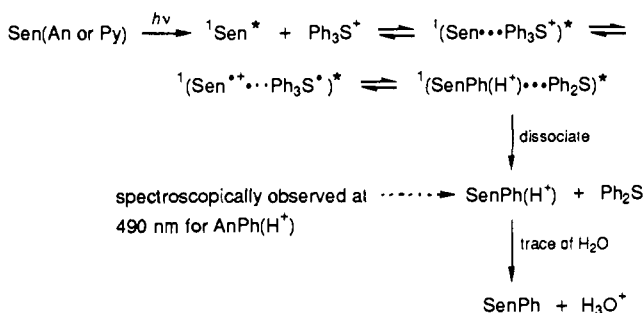


Figure 10. Transient photobleaching signal at 620 nm of (3-(9-anthracenyl)propyl)diphenylsulfonium hexafluoroantimonate (2×10^{-4} M) and 5×10^{-5} M sodium bromocresol green in methanol.

toproduced protons in methanol is much faster than that in acetonitrile. Figure 11A shows the transient spectrum of triplet excited acetone sensitized decomposition of Ph_2SSbF_6 in N_2 -saturated acetonitrile. A broad absorption band is observed at 760 nm, due to Ph_2S^{*+} .¹⁶ Figure 11B shows the time-resolved

Scheme I. Singlet Sensitization of Triphenyl Sulfonium Cation via An or Py, a Charge-Transfer Reaction



signal at 760 nm under nitrogen- and air-saturated conditions. Air, a typical triplet scavenger, removes the acetone triplet and the 760 nm signal, confirming that the sensitization process is due to the triplet excited state, which is very sensitive to trace amounts of oxygen. Figure 11C shows the dye photobleaching signal at 620 nm and the transient absorption signal at 760 nm of Ph_2S^{*+} . These data show that the rate of photoproducted protons matches that of the decay of Ph_2S^{*+} in the ${}^3\text{acetone}^*-\text{Ph}_3\text{SSbF}_6/\text{CH}_3\text{CN}$ system.

Mechanism. To summarize our studies and to compare our data with previous studies, we postulate Scheme I for the photolysis of sulfonium salts.

Electron transfer from excited arene to triphenylsulfonium salt to yield Ar^{*+} has been reported by Pappas et al.¹⁷ Recently, Sahyun et al. and Hacker et al.¹⁸ also reported that phenylated arene photoproducts are produced from an "in-cage" rearrangement mechanism. Phenylthiobiphenyl isomers are also produced in system where the oxidation potential E_{ox} of the Ar is greater than 1.31 V (i.e., the E_{ox} of Ph_2S in CH_3CN).¹⁹ Regarding the present studies, anthracene and pyrene both possess E_{ox} values less than that of Ph_2S ; i.e., 1.09 and 1.16 V, respectively.²⁰ Therefore, in-cage oxidation of Ph_2S by Ar^{*+} is energetically forbidden, which eliminates the formation of phenylthiobiphenyl isomers. Under these conditions, in-cage phenyl radical migration to the Ar^{*+} , giving a proton-rich phenylated arene ($\text{PhAr}(\text{H}^+)$), produces the photoproducted protons, and proton release is enhanced by trace amounts of water. The transient species absorbing around 490 nm, as shown in the insert in Figure 4A, is assigned to $\text{PhAn}(\text{H}^+)$. This is supported by the following arguments: (a) the species is cationic in character (i.e., quenched by I^- at the diffusion-controlled limit but not quenched by oxygen, an anion and radical quencher); (b) the species is not An^{*+} as shown in Figures 4B and 5B, where the An^{*+} (700 nm) decays much more slowly than the 490-nm species; (c) the species is the precursor of the photoproducted protons and is quenched by water, and the decay of this species with different $[\text{H}_2\text{O}]$ matches the rate of proton formation (pH-jump experiments, vide ante); (d) it is not a nitrile-trapped cation, because the spectrum with benzonitrile shows no difference from that in acetonitrile; and (e) the final stable photoproduct of this species, a phenylated anthracene product, is isolated by HPLC and identified by both steady-state and time-resolved fluorescence.

A similar kinetic scheme is also suggested for the photodecomposition of (3-(9-anthracenyl)propyl)diphenylsulfonium salt after UV irradiation (>375 nm). This is also supported by the findings that (a) the products exhibit UV absorption and fluorescence spectra that are quite similar to the spectra for phenylated anthracene,²¹ (b) the fluorescence lifetime and quantum yield increased after UV (>375 nm) irradiation, and, most importantly, (c) phenylated anthracene derivative products are isolated by HPLC and identified by both steady-state and time-resolved fluorescence, which indicates a transition from alkyanthracene derivatives to phenylanthracene derivatives. The results support in-cage rearrangement of a phenyl group to anthracene. In fact, Saeva et al.²² have reported that, on the basis

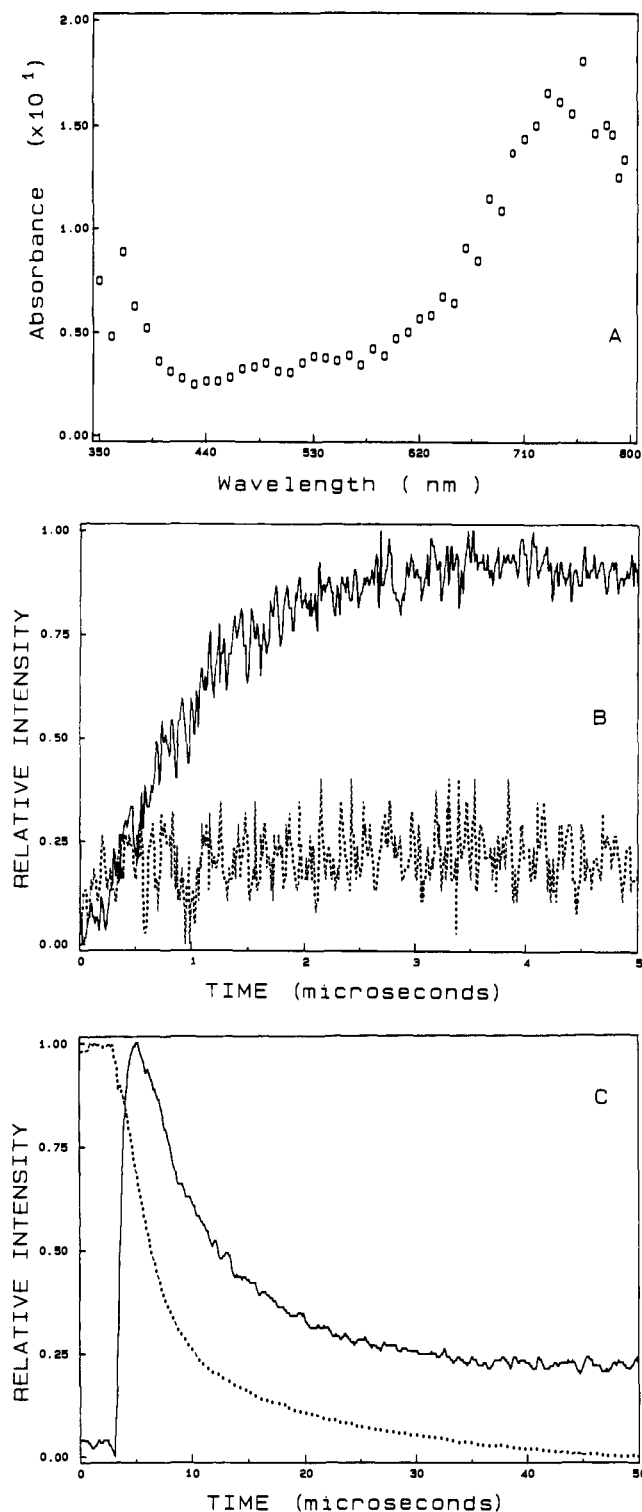
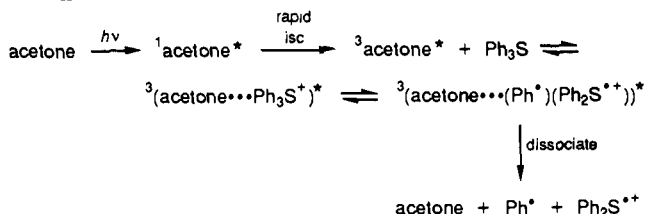


Figure 11. (A) Transient absorption spectrum of Ph_3SSbF_6 in nitrogen-saturated CH_3CN sensitized by triplet acetone. (B) Effect of air on the time-resolved transient absorption at 760 nm of (A): (solid line) nitrogen-saturated solution; (dashed line) air-saturated solution. (C) Comparison of the time-resolved transient absorption signal of $\text{Ph}_2\text{S}^{+\bullet}$ at 760 nm (solid line) and the photobleaching signal of bromocresol green at 620 nm (dotted line).

of the photoproduct analysis, this type of in-cage rearrangement indeed occurs on photolysis of anthrylsulfonium salts in CH_3CN .

In addition, our observation of the transient species at 490 nm is in agreement with the earlier observation by Sahyun et al., but they incorrectly assigned it to dialkoxyanthracene radical cation.²³

Scheme II. Triplet Sensitization of Triphenylsulfonium Cation via Acetone



Further supports of assigning this 490-nm species as $\text{PhAn}(\text{H}^+)$ in the ${}^1\text{An}^*$ electron transfer to Ph_3S^+ in CH_3CN is that Hacker et al. proposed a transient species $\text{PhS-Ph}(\text{Ph})(\text{H}^+)$ ($\lambda_{\text{max}} = 465$ nm, $\tau_{1/2} = 11$ μs in CH_3CN) in their photo-CIDNP studies,²⁴ in which not only the absorption spectral region but also the half-life are similar to our data.

Hacker et al.⁴ reported that triplet sensitization of triphenylsulfonium salt by excited ketone ($k_T > 75$ kcal/mol) yielded products that originated from $\text{Ph}_2\text{S}^{+\bullet}$. We observed spectroscopically the formation of $\text{Ph}_2\text{S}^{+\bullet}$ in ${}^3\text{acetone}^*$ ($k_T = 74$ kcal/mol) sensitized Ph_3SSbF_6 in acetonitrile as shown in Figure 11, and this supports their conclusion. Based on spin conservation, the products of a triplet complex (such as ${}^3(\text{acetone} \cdots \text{Ph}_3\text{S}^+)^*$ in Scheme II) will have a total electron spin that is triplet. Our time-resolved studies suggest a mechanism as shown in Scheme II for triplet acetone sensitization of triphenylsulfonium salts. Further reactions of $\text{Ph}_2\text{S}^{+\bullet}$ with solvent or trace amount of water generate protons.

Conclusion

Nanosecond time-resolved spectroscopy and pH-jump studies were employed to illustrate the mechanisms of photodecomposition of triphenylsulfonium hexafluoroantimonate via ${}^1\text{arene}^*$ electron transfer or ${}^3\text{acetone}^*$ sensitization in methanol and acetonitrile. In addition, direct excitation of (3-(9-anthracenyl)propyl)diphenylsulfonium hexafluoroantimonate in both methanol and acetonitrile are also studied. In the time-resolved study, the data show no formation of $\text{Ph}_2\text{S}^{+\bullet}$ in ${}^1\text{An}^*$ or ${}^1\text{Py}^*$ electron transfer to triphenylsulfonium cation and are in agreement with the fact that arenes with an $E_{\text{ox}} < 1.31$ V (E_{ox} of Ph_2S in CH_3CN) cannot oxidize Ph_2S to $\text{Ph}_2\text{S}^{+\bullet}$. Further reaction of this cation (i.e., $\text{Ph}_2\text{S}^{+\bullet}$) with Ph^* radical (in-cage) could give phenylthiobiphenyl isomers. Under the condition that the Ar has $E_{\text{ox}} < 1.31$ V, Ph^* can migrate to the $\text{Ar}^{+\bullet}$ and form a proton-rich phenylated arene ($\text{Ph-Ar}(\text{H}^+)$), which serves as a source of photoproducted protons. This transitory species, $\text{Ph-An}(\text{H}^+)$, is observed spectroscopically (absorbs ~ 490 nm) in both ${}^1\text{An}^*$ electron transfer to triphenylsulfonium cation and direct excitation of (3-(9-anthracenyl)propyl)diphenyl sulfonium hexafluoroantimonate in acetonitrile. Iodide ion quenches the cationic species at the diffusion-controlled limit ($k_q \sim 10^{10}$ M^{-1} s^{-1}), while water quenches it with $k_q \sim 10^6$ M^{-1} s^{-1} . ${}^3\text{Acetone}^*$ sensitization of triphenylsulfonium hexafluoroantimonate in acetonitrile produces $\text{Ph}_2\text{S}^{+\bullet}$, which is observed spectroscopically at ~ 760 nm by time-resolved spectroscopy. pH-jump data show that the formation of photoproducted protons is slow in anhydrous aprotic solvent, such as acetonitrile (i.e., microseconds); however, the formation rate is markedly increased in protic solvents such as methanol (<200 ns) or upon addition of water to the anhydrous acetonitrile.

The major use of this system is in photoimaging by H^+ cross-linking of epoxide films (i.e., Quatex 1010). To this end, our measurements show that H^+ production in solution is fast and that H^+ mobility in rigid epoxide film is slow. Reaction of H^+ with the dye, pH indicator, takes days at 20 °C and hours at 70 °C.²⁵

(23) (a) DeVoe, R. J.; Sahyun, M. R. V.; Schmidt, E.; Sharma, D. K. *Can. J. Chem.* **1990**, *68*, 612-619. (b) Sahyun, M. R. V.; DeVoe, R. J.; Sharma, D. K. *Mol. Cryst. Liq. Cryst.* **1991**, *194*, 325-330.

(24) Welsh, K. M.; Dektar, J. L.; Hacker, N. P.; Turro, N. J. *Polym. Mater. Sci. Eng.* **1989**, *61*, 181-184.

(22) Saeva, F. D.; Breslin, D. T. *J. Org. Chem.* **1989**, *54*, 712-714.

Acknowledgment. We would like to thank IBM Corp. and National Science Foundation for financial support of this work and Dr. Sahyun at 3 M for a helpful discussion. Joe Kuczynski would like to thank Dr. S. P. Pappas for the synthetic procedures

for (3-(9-anthracenyl)propyl)diphenylsulfonium hexafluoroantimonate.

Registry No. Ph₃SSbF₆, 57840-38-7; Ph-An(H⁺), 62726-22-1; (3-(9-anthracenyl)propyl)diphenylsulfonium, 132399-87-2; sodium bromocresol green, 67763-24-0; pyrene, 129-00-0; anthracene, 120-12-7; (3-(9-anthracenyl)propyl)diphenylsulfonium hexafluoroantimonate, 132399-88-3.

(25) Chu, D. Y.; Iu, K.-K.; Thomas, J. K. IBM subcontract, 1990-1991.

Hydrothermal Synthesis of K₂PdSe₁₀. Coexistence of Two Large Interpenetrating Three-Dimensional Frameworks of [Pd(Se₄)₂]²⁻ and [Pd(Se₆)₂]²⁻

Kang-Woo Kim and Mercuri G. Kanatzidis*

Contribution from the Department of Chemistry and Center for Fundamental Materials Research, Michigan State University, East Lansing, Michigan 48824. Received October 9, 1991

Abstract: The hydrothermal reaction of PdCl₂ with K₂Se₄ in the presence of different KOH and water in the 1:5:5:40 ratio produced K₂[PdSe₁₀] (I), the first metal polychalcogenide compound containing two interpenetrating three-dimensional frameworks. The black rectangular chunky crystals of I are insoluble in water and most organic solvents. They crystallize in the orthorhombic space group I2₁2₁2₁ (no. 24) with *a* = 15.872 (9) Å, *b* = 15.922 (9) Å, *c* = 12.885 (8) Å, *V* = 3256 (6) Å³. I is composed of two independent interpenetrating 3D diamond-like frameworks of [Pd(Se₄)₂]²⁻ and [Pd(Se₆)₂]²⁻. Each framework contains large tunnels running parallel to the *a*- and *b*-crystallographic axes. The coordination geometry around Pd is square-planar. The average Pd-Se and Se-Se distances are 2.462 (5) and 2.35 (2) Å, respectively. The closest distances between K⁺ ions and Se atoms are in the range of 3.27 (2) and 3.75 (2) Å.

Introduction

Recently, we showed that hydrothermal synthesis can be applied to the preparation of some novel Mo polychalcogenide compounds.¹ In order to explore the generality of the technique for other metals, we turned our attention to the more chalcophilic late transition elements. The reactions of such elements with Q_x²⁻ ligands have been explored to some extent at ambient temperature and pressure and were found to produce a number of interesting *molecular* compounds.² In the case of the cation/M/Q (M = Cu, Ag; Q = S, Se) and cation/Hg/Te systems it was found that some cations stabilize *polymeric* one-dimensional structures such as those of (Ph₄P)[Ag(Se₄)],³ (Me₄N)[Ag(Q₃)],⁴ (Q = S²⁻, Se²⁻), (H₃NC-H₂CH₂NH₃)[Cu(S₅)₂],⁵ and (Ph₄P)₂[Hg₂Te₅].⁶ This raises possibilities for other interesting polychalcogenide-based polymeric structures containing various metals. A particular set of coun-

terions from which it is difficult to obtain pure crystalline products from solution are the alkali metals. Furthermore, based on a significant body of experimental evidence the importance of counterion in determining the structure of the [MQ_x]ⁿ⁻ anion has now been recognized.^{2,3} For example, we have shown that minor modifications in the size of the counterion (R₄N⁺, Ph₄P⁺, K⁺, Cs⁺) can cause major geometric and electronic reorganization of the anionic structure of silver and gold polyselenide compounds.³ This motivated us to explore new counterions (e.g., alkali ions) in search of new [MQ_x]ⁿ⁻ structure types, particularly polymeric. Since we often encounter difficulties in isolating crystalline polymeric compounds using ambient temperature and pressure conditions, we resorted to the hydrothermal technique. The palladium chemistry seemed particularly attractive for such exploration because its first polysulfide compound (NH₄)₂[PdS₁₁]⁷ was reported to have a polymeric layered structure with S₅²⁻ and S₆²⁻ ligands. The corresponding polyselenide chemistry is unknown, and based on previous experience we expect it to be different. Herein we report the hydrothermal synthesis and structural characterization of K₂[PdSe₁₀] (I), a compound with an intriguing three-dimensional (3D) architecture composed of two unprecedented interpenetrating frameworks. The extended structure of I is rationalized on the basis of anion-cation packing interactions.

Experimental Section

All work was done under a nitrogen atmosphere. PdCl₂ was purchased from Alpha Products Inc. Potassium tetraselenide K₂Se₄ was prepared in liquid ammonia from potassium metal and elemental selenium in a 2:4 ratio as described previously.³ The X-ray powder diffraction patterns were recorded with a Phillips XRG-3000 computer controlled powder

(1) (a) Liao, J.-H.; Kanatzidis, M. G. *J. Am. Chem. Soc.* **1990**, *112*, 7400-7402. (b) Liao, J.-H.; Kanatzidis, M. G. *Inorg. Chem.* **1992**, *31*, 431-439. (c) Park, Y.; Liao, J.-H.; Kim, K.-W.; Kanatzidis, M. G. In *Inorganic and Organometallic Polymers and Oligomers*; Harrod, J. F., Laine, R. M. Eds.; Kluwer Academic Publishers: 1991; pp. 263-276.

(2) (a) Kanatzidis, M. G. *Comments Inorg. Chem.* **1990**, *10*, 161-195. (b) Ansari, M. A.; Ibers, J. A. *Coord. Chem. Rev.* **1990**, *100*, 223-266. (c) Kolis, J. W. *Coord. Chem. Rev.* **1990**, *105*, 195-219.

(3) (a) Huang, S.-P.; Kanatzidis, M. G. *Inorg. Chem.* **1991**, *30*, 1455-1466, and references therein. (b) Park, Y.; Kanatzidis, M. G. *Angew. Chem., Int. Ed. Engl.* **1990**, *29*, 914-915. (c) Kanatzidis, M. G.; Huang, S.-P. *Angew. Chem., Int. Ed. Engl.* **1989**, *28*, 1513-1514. (d) Liao, J.-H.; Kanatzidis, M. G., submitted for publication. (e) Kim, K.-W.; Kanatzidis, M. G. submitted for publication.

(4) Banda, R. M. H.; Craig, D. C.; Dance, I. G.; Scudder, M. L. *Polyhedron* **1989**, *8*, 2379-2383.

(5) Kiel, G.; Gattow, G.; Dingeldein, T. Z. *Anorg. Allg. Chemie* **1991**, *596*, 111-119.

(6) Haushalter, R. C. *Angew. Chem., Int. Ed. Engl.* **1985**, *24*, 432-433.

(7) Haradem, P. S.; Cronin, J. L.; Krause, R. L.; Katz, L. *Inorg. Chim. Acta* **1977**, *25*, 173-179 and references therein.